

# Assessment of LES models for a fully developed wind-turbine array boundary layer

D.Folch, F.X.Trias, A.Oliva

Heat and Mass Transfer Technological Center, Technical University of Catalonia  
C/Colom 11, 08222 Terrassa (Barcelona)

<http://www.cttc.upc.edu/>

[david.folch@upc.edu](mailto:david.folch@upc.edu) [francesc.xavier.trias@upc.edu](mailto:francesc.xavier.trias@upc.edu) [asensio.oliva@upc.edu](mailto:asensio.oliva@upc.edu)

**Abstract** – Direct numerical simulations of the incompressible Navier-Stokes equations at high Reynolds numbers are not yet feasible, so dynamically less complex mathematical formulations such as Large Eddy Simulation (LES) have been developed. For the well-known eddy-viscosity models for LES, the computational method is based on the combination of invariants of a symmetric tensor that depends on the gradient of the resolved velocity field,  $G = \nabla \bar{u}$ . Brand-new models (namely S3PQR) have been developed using the first three principal invariants of the symmetric tensor  $GG^T$  with excellent results. Therefore, in this work, we will focus on the application of the S3PQR and other LES models on the free boundary layer case. Then, we will test their performances over a fully developed boundary layer wind farm, using a simplified model of a wind turbine.

## 1. Introduction

Large Eddy Simulation (LES) equations result from applying a spatial filter to the incompressible Navier-Stokes equations, yielding:

$$\begin{aligned} \partial_t \bar{u} + C(\bar{u}, \bar{u}) &= D(\bar{u}) - \nabla p - \nabla \cdot \tau(\bar{u}); \\ \nabla \cdot \bar{u} &= 0 \end{aligned} \quad (1)$$

where  $\bar{u}$  is the filtered velocity and  $\tau(\bar{u})$  is the subgrid stress (SGS) tensor that approximates the effect of the under-resolved scales.

This equation needs a closure model in order to be numerically solved. The LES closure is of the type  $\tau(\bar{u}) \approx -2\nu_e S(\bar{u})$  where  $S(\bar{u}) = 1/2(\nabla \bar{u} + \nabla \bar{u}^T)$  is the rate-of-strain tensor. We must define an eddy viscosity:  $\nu_e = (C_m \Delta)^2 D_m(\bar{u})$  where  $C_m$  is the model constant,  $\Delta$  is the subgrid characteristic length, and  $D_m(\bar{u})$  is the differential operator with units of frequency associated with the model [1].

The S3PQR models involve invariants of the symmetric tensor  $GG^T$ . The different types of S3PQR models are obtained by restricting them to solutions with only two of those invariants [2]. The three different obtained models are  $\nu_e^{S3PQ}$ ,  $\nu_e^{S3PR}$ ,  $\nu_e^{S3QR}$  or for simplicity, PQ, PR, QR. There are two ways to determine the model constant:

1. Imposing numerical stability and less or equal dissipation than Vreman's model. Then,

$$C_{s3pq} = C_{s3pr} = C_{s3qr} = \sqrt{3}C_{Vr} \approx 0.458$$

2. Granting that the averaged dissipation of the models is equal to that of the Smagorinsky model. Then,

$$C_{s3pq} = 0.572, C_{s3pr} = 0.709, C_{s3qr} = 0.762$$

Therefore, there are six possible combinations to test (3 model types x 2 constants) that we will call PQ1, PQ2, and so on. The general algorithm for a boundary layer is based on the method proposed by Spalart and Leonard (1987) [3], which includes normal coordinate similarity transformations, growing terms  $GT(\bar{u}, \bar{U})$  and scaling factors.

There are some differences with our (pseudo-spectral) implementation, though. First, our algorithm is based on the strong formulation of the Navier-Stokes equations with a Poisson - pressure correction term. Second, we use the standard algebraic scaling [4],  $y_\infty = L \frac{1+y}{1-y}$ , for the semi-infinite domain over the normal direction. Finally, the computation relies on a fully explicit second-order time-integration method [5]. We will test the zero mean pressure gradient case.

## 2. Model Deployment and First Results

For all the current computations, the grid size of the domain is  $N_x = 32$ ,  $N_y = 64$ , and  $N_z = 32$  points, where  $x$ ,  $y$ , and  $z$ , are the streamwise, wall-normal, and spanwise directions. The Reynolds number is fixed along the simulation to  $Re_\delta = 1000$ , where  $\delta$  is the displacement thickness.

### 2.1 Boundary layer

First, we deal with the free boundary layer cases without the turbine model. To compare the LES models and the Spalart and Leonard (1987) [3] results, we can list three main parameters:  $u_\tau$  as the friction velocity,  $H$  as the ratio of the displacement thickness to the momentum thickness, and  $\kappa$  as the Von Kármán constant (see Table 1, where Sp-Le stands for the reference values).

Table 1: boundary layer characteristic parameters calculated for each model

Case:	Sp-Le	No model	Vreman	WALE	PQ1	PR1	QR1	<b>PQ2</b>	PR2	QR2
$u_\tau$	0.049	0.048	0.047	0.046	0.048	0.049	0.049	<b>0.047</b>	0.047	0.048
$H$	1.52	1.57	1.57	1.55	1.57	1.55	1.56	<b>1.56</b>	1.57	1.56
$\kappa$	0.39	0.36	0.45	0.44	0.36	0.40	0.37	<b>0.36</b>	0.36	0.39

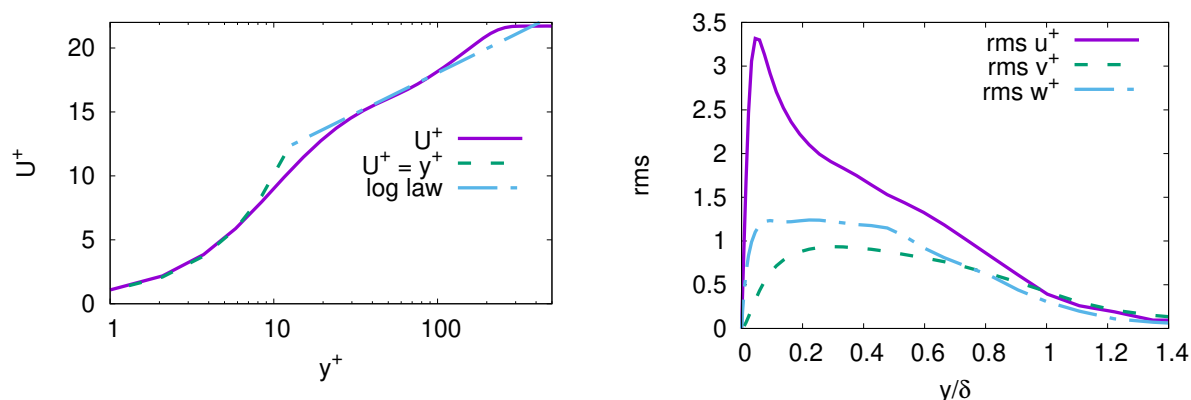


Figure 1: Case PQ2, present results. Left: normalized average streamwise velocity profile,  $U^+$ ; log law;  $U^+ = y^+$ . Right:  $\text{rms } u^+$ ;  $\text{rms } v^+$ ;  $\text{rms } w^+$

The Smagorinsky method did not yield meaningful results with the current algorithm (incorrect near-wall behavior). The rest of LES models give reasonable results, with PQ2 standing by now as the best in the global analysis. As an example of the performance of PQ2, we plot

the velocity profile and the root mean square of the velocities (figure 1). Thus so far we have obtained reliable results with low computational effort for the free boundary layer.

## 2.2 Wind farm

We will follow the model stated by [6] which is based on the concept of a disk actuator for every wind turbine. The force of the turbine (per unit mass), in the streamwise direction, at a given grid point  $i, j, k$ , is given by

$$F(i, j, k) = -\frac{1}{2}C_T' \langle \bar{u}^T \rangle_d^2 \frac{\gamma_{j,k}}{\Delta x}$$

where  $C_T'$  is a thrust coefficient,  $\langle \bar{u}^T \rangle_d^2$  is the disk averaged local velocity,  $\gamma_{j,k}$  is the fraction area overlap of the disk and  $\Delta x$  is the distance between turbines. This disk actuator model can be straightforwardly applied to our algorithm. We will compute our wind farm with the same number and array geometry of the turbines that a specific case of the reference: 24 disk actuators evenly distributed in four rows and six columns.

However, all the other configuration parameters, like the Reynolds number, the supply of energy, and the wall boundary conditions, are far different. So, at this moment the comparison can only rely on the general behavior of the vertical profiles and the magnitude orders of the values. We will show here only the results for the PQ2 algorithm. The complete comparison between all the models will be presented in the full-length paper.

Some of the several quantities that may be of interest are listed in Table 2. The meaning of the terms are as follows:  $z0_{Hi}/zH$ , as the ratio of the effective roughness above the turbine hub and the height of the turbines' center;  $u_\tau$ , the usual friction velocity at the wall;  $u_*$ , the computed friction velocity above the hub;  $P$ , the time and horizontally averaged power extracted for every turbine;  $W_t$ , the time, horizontally, and vertically (along the hub) averaged power. Finally, the term EB (for energy budget) is the balance between all the energy contribution terms. For a perfect match, it should be 100% (the reference achieves 98%).

Table 2: some computed useful quantities of a wind farm simulation

PQ2	$z0_{Hi}/zH$	$u_\tau$	$u_*$	$u_\tau/u_*$	$P/u_*^3$	$W_t/u_*^3$	EB
Results	0.176	0.053	0.115	0.46	0.68	0.83	93%

As shown in [6], we can expect the presence of two well-defined log laws along the vertical velocity profile. In Figure 2, it can be seen that this condition is fulfilled. Moreover, the different terms of the energy budget shown at the right of this Figure 2 follow the same patterns as the reference. Therefore, the S3PQR algorithms are well-suited to be applied to wind farm simulations.

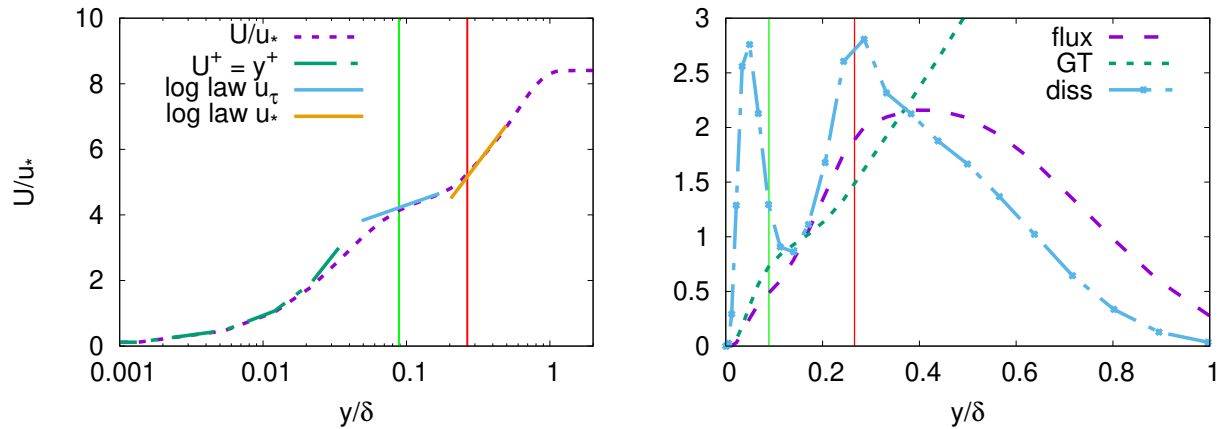


Figure 2: Left: average streamwise velocity. The green vertical line is the position of the bottom of the turbine hub. The red line is the top. Note the law of the wall, and the two log laws. Right: Normalized mean kinetic energy contributions: **flux**,  $-\langle uv \rangle U/u_*^3$ ; **GT**, normalized growing terms; **diss**,  $-\langle uv \rangle \partial_y U / (u_*^3/\delta)$

## References

1. F. Nicoud, H. B. Toda, O. Cabrit, S. Bose, and J. Lee, “Using singular values to build a subgrid-scale model for large eddy simulations,” *Physics of Fluids*, vol. 23, no. 8, p. 085106, 2011.
2. F. X. Trias, D. Folch, A. Gorobets, and A. Oliva, “Building proper invariants for eddy-viscosity subgrid-scale models,” *Physics of Fluids*, vol. 27, no. 6, p. 065103, 2015.
3. P. Spalart and A. Leonard, *Direct Numerical Simulation of Equilibrium Turbulent Boundary Layers*. Berlin: Springer-Verlag, 1987.
4. J. P. Boyd, *Chebyshev and Fourier Spectral Methods*. Dover Publications, Inc., 2001.
5. F. X. Trias, D. Folch, A. Gorobets, and A. Oliva, “Spectrally-consistent regularization of Navier-Stokes equations,” *Journal of Scientific Computing*, vol. 79, pp. 992–1014, 2019.
6. M. Calaf, C. Meneveau, and J. Meyers, “Large eddy simulation study of fully developed wind-turbine array boundary layers,” *Physics of Fluids*, vol. 22, p. 015110, 2010.